Self-Assembly

DOI: 10.1002/ange.201308792

Multifunctional Porous Microspheres Based on Peptide–Porphyrin Hierarchical Co-Assembly**

Qianli Zou, Lu Zhang, Xuehai Yan, Anhe Wang, Guanghui Ma, Junbai Li, Helmuth Möhwald, and Stephen Mann**

Abstract: *Photocatalytically active, multi-chambered, biomolecule-based microspheres were prepared by hierarchical co-assembly of simple dipeptides and porphyrins. The colloidal microspheres are highly hydrated and consist of a network of J-aggregate nanoscale substructures that serve as light-harvesting antennae with a relatively broad spectral cross-section and considerable photostability. These optical properties can be exploited in photocatalytic reactions involving inorganic or organic species. Taken together, these structural and functional features suggest that soft porous biomolecule-based colloids are a plausible photosynthetic model that could be developed towards demonstrating aspects of primitive abiotic cellularity.*

The hierarchically ordered co-assembly of molecular and supramolecular building blocks (such as peptides, proteins, lipids, nucleic acids, and saccharides) in living organisms is a fundamental organizational principle of cellular systems.[1] From a biomimetic perspective, the design and construction of primitive cell-like architectures in the laboratory represents an important step towards modeling key aspects of prebiotic chemistry[1c,2] and advancing the synthesis of integrated microscale materials.[3] Typically, ensembles of biological components are encapsulated within self-assembled membrane-bound vesicles or semi-permeable capsules prepared from fatty acids,[4,5] phospholipids,[6] proteins,[7] and inorganic nanoparticles,[8] and various complex transformations such as gene expression,[3b,6d,8a] template-directed replication,[3b,5,6c] enzyme catalysis,[8,9] and proto-cytoskeletal assembly.[6b,8b] Alternatively, simpler membrane-free models of abiotic cellularity have been recently constructed by binary combinations of cationic oligopeptides and anionic mononucleotides associated with liquid–liquid phase separation.[10] Another possible strategy to construct new architectures for synthetic cellularity could involve small biomolecule combinations and their cooperative self-assembly. To the best of our knowledge, there are no known examples of such structural architechtures with multifunctional properties self-assembled by biological and potentially prebiotically combinations between key small molecules such as amino acids, small peptides, mononucleotides, and porphyrins.

Herein, we investigate the feasibility of preparing porous multi-chambered, biomolecule-based microspheres by electrostatically induced spontaneous co-assembly in water of a dipeptide (diphenylalanine, L-Phe-L-Phe, FF; see Figure S1 in the Supporting Information)[11] and sulfonated porphyrin (tetrakis(4-sulfonatophenyl)porphine, $[H_2TPPS]$ ($[H_2TPPS]^{4-}$ in neutral solution); Figure S1),[12] both of which represent plausible classes of prebiotic compounds.[13] In acidic solution, the dipeptide is in the form of a singly charged cation ($[FF]^+$) arising from protonation of the terminal primary amine, whilst the porphyrin is dianionic ($[H_4TPPS]^{2-}$) because of deprotonation of the four sulfonic acid groups and protonation of the pyrrole nitrogen atoms. We demonstrate that dispersions of microspheres can be readily produced from stoichiometric mixtures of $[FF]^+$ and $[H_4TPPS]^{2-}$. The microspheres are porous and consist of a water-filled multi-chambered interior that is accessible to guest molecules, and which comprises an interconnected and self-supporting network of peptide–porphyrin nanorods. Significantly, the nanorods consist of supramolecular stacks of porphyrin molecules (J-aggregates) along with electrostatically integrated dipeptides, and as a consequence capture light when irradiated and remain stable against photodegradation. We exploit these light-harvesting properties and the subsequent conversion into chemical energy to undertake various photocatalytic transformations associated specifically with the peptide–porphyrin microspheres. Taken together, our results demonstrate a new type of multifunctional colloidal co-assembly based on small biomolecules. This probably offers a simple, energy sustainable biomimetic model that could be potentially developed towards studying aspects of primitive abiotic cellularity with light as an energy source.

[*] Dr. Q. Zou, Prof. Dr. X. Yan, Prof. Dr. G. Ma
National Key Laboratory of Biochemical Engineering
Institute of Process Engineering
Chinese Academy of Sciences, 100190 Beijing (China)
E-mail: yanxh@home.ipe.ac.cn
Dr. L. Zhang, Prof. Dr. H. Möhwald
Max Planck Institute of Colloids and Interfaces
Am Mühlenberg 1, 14476 Potsdam/Golm (Germany)
Dr. A. Wang, Prof. Dr. J. Li
Beijing National Laboratory for Molecular Sciences (BNLMS)
Key Lab of Colloid and Interface Sciences
Institute of Chemistry, Chinese Academy of Sciences
100190 Beijing (China)
Prof. Dr. S. Mann
Centre for Organized Matter Chemistry, School of Chemistry
University of Bristol, Bristol BS8 1TS (UK)
E-mail: s.mann@bristol.ac.uk

[**] X.Y. acknowledges support of the Talent Fund from the Recruitment Program of Global Youth Experts and for a research fellowship from the Alexander von Humboldt Foundation. The authors acknowledge financial support from the Chinese Academy of Sciences, the CAS visiting professorship for senior international scientists (grant number 2013T2G0037), German Max-Planck Society, and the ERC (advanced grant scheme).

Supporting information for this article is available on the WWW under http://dx.doi.org/10.1002/anie.201308792.

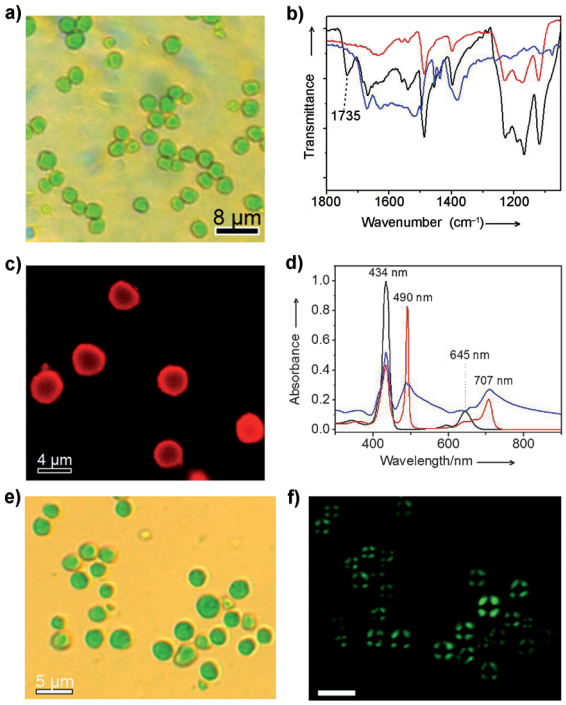

Figure 1. Formation and structural analysis of peptide–porphyrin microspheres. a) Optical image showing dispersion of bright green microspheres. b) FTIR spectra of $[H_2TPPS]$ powder (red), FF peptide (blue), and peptide–porphyrin microspheres (black). An additional absorption band at 1735 cm^{-1} corresponding to the free -COOH group of FF is observed for the peptide–porphyrin microspheres. c) Confocal image of microspheres showing autofluorescence; samples were excited at 488 nm and the emitted fluorescence collected from 680–760 nm. d) UV/Vis absorption spectra of aqueous $[H_2TPPS]^{4-}$ at neutral pH (black), dispersion of J-aggregates (stacked $[H_4TPPS]^{2-}$) at pH 1.9 (red), and peptide–porphyrin microspheres assembled by electrostatic coupling of cationic $[FF]^+$ and dianionic $[H_4TPPS]^{2-}$ (blue). e) Bright-field image and f) polarized image of microspheres showing strong anisotropic photoluminescence attributed to birefringence when placed between crossed polarizers (the scale bar is 5 μm).

Aqueous solutions of $[FF]^+$ and $[H_4TPPS]^{2-}$ were mixed at a final pH value smaller than 2 to produce a bright green dispersion consisting of peptide–porphyrin microspheres with a $[FF]^+$: $[H_4TPPS]^{2-}$ molar ratio of 2.3:1 (Figure 1a). In general, the microspheres formed within 1 h of mixing. The stoichiometry is consistent with the formation under acidic conditions of a close to charge-neutralized 2:1 dipeptide–porphyrin ionic complex. Fourier transform infrared (FTIR) spectra of the microspheres reveal characteristic bands for both FF and porphyrin components, as well as an additional absorbance at 1735 cm^{-1} (Figure 1b), attributed to the C=O stretching vibration of a non-hydrogen-bonded -COOH group.[14] This implies that the free carboxy groups do not involve interactions with $[H_4TPPS]^{2-}$, in turn suggesting the predominance of electrostatic interaction for formation of microspheres. Confocal fluorescence microscopy images show red autofluorescence that is attributed to the presence of the porphyrin in the microspheres (Figure 1c and Figure S2). The images often exhibit increased levels of fluorescence intensity towards the periphery of the microspheres, suggesting that the microstructure is heterogeneous. Moreover, strong anisotropic photoluminescence (birefringence) was observed when the dispersion was placed between crossed polarizers (Figure 1e,f), indicating the presence of ordered arrays of $[H_4TPPS]^{2-}$ anions within the peptide–porphyrin microspheres. This is in agreement with UV/Vis absorption spectra that show red-shifted Soret and Q bands at 490 and 707 nm, respectively, which are typical of J-aggregates comprising slipped face-to-face stacked arrays of $[H_4TPPS]^{2-}$ dianions (Figure 1d).[15] However, both the Soret and Q bands are extensively broadened compared with the same peaks observed for a dispersion of pure J-aggregates, suggesting that the supramolecular organization is partially disordered by interactions between the cationic dipeptide and dianionic $[H_4TPPS]^{2-}$.

Scanning electron microscopy (SEM) images confirm the formation of relatively uniform microspheres with diameters of 3–5 μm (Figure 2a and Figure S3). High-magnification images indicate that the microspheres have a roughened surface texture that appears to comprise an agglomerated network of discrete subunits. This is confirmed by transmission electron microscopy (TEM) and atomic force microscopy (AFM), which show the presence of a disordered array of nanorods (Figure 2b,c and Figure S4). The nanostructures are tens of nanometers in height and hundreds of nanometers in length (Figure 2d). SEM images of freeze-fractured microspheres reveal a porous, multi-chambered interior with compartments ranging from several to hundreds of nanometers in dimension (Figure 2e and Figure S5). The high level of internalized porosity is consistent with thermogravimetric analysis (TGA) and differential scanning calorimetry (DSC), indicating that the microspheres consist of

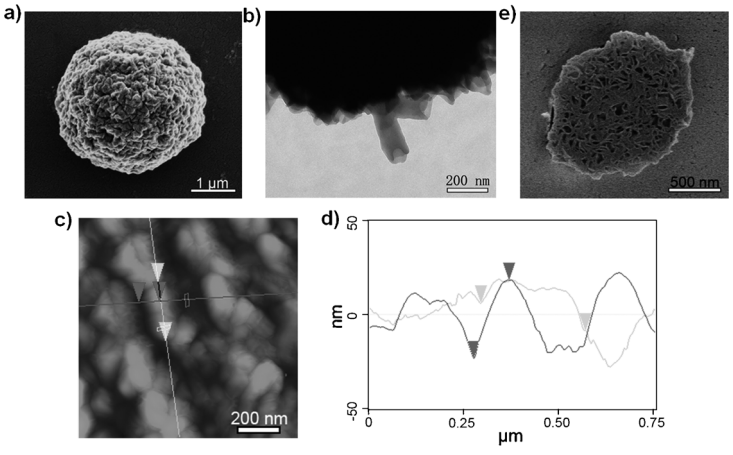

Figure 2. Morphological analysis of peptide–porphyrin microspheres. a) SEM image of a single microsphere showing irregular surface texture. b) TEM image of a microsphere showing a substructure of aggregated nanorods and nanotubes. c) AFM contact-mode height image with line profiles (light gray and gray lines) showing the presence of closely packed nanorods; and d) corresponding height profiles confirming the presence of elongated nanostructures on the microsphere surface (x axis: distance, y axis: height). e) SEM image of a single microsphere cross-section showing porous, multi-chambered interior.

approximately 90 wt% water (Figure S6 in the Supporting Information). Formation of uniformly sized microspheres with multichambers may be attributed to the competition between long-range electrostatic repulsion and short range van der Waals attraction. During assembly of nanorods into microspheres in solution, within these spheres there could be reorganization of the $[FF]^+$ and $[H_4TPPS]^{2-}$ charged building blocks. These would prefer to be at the periphery due to electrostatic repulsion, thus leading to a multicompartment structure.

UV/Vis spectroscopy was used to elucidate the pathway responsible for microsphere assembly, which in general occurred within a period of 1 hour at room temperature (increases in turbidity were often observed after 30 minutes). The spectra indicate that $[H_4TPPS]^{2-}$ J-aggregates are formed almost instantaneously upon acidification in the presence of $[FF]^+$, and continue to increase in size during a further period of 12 minutes as evidenced by a progressive increase in the intensity of the 490 nm peak (Figure 3a). The observations are attributed to dipeptide-mediated growth of the J-aggregates over this initial time period to produce a dispersion of peptide–porphyrin nanorods. Subsequent aggregation of the nanorods to produce the microspheres is associated with a concomitant decrease and broadening of the J-aggregate Soret and Q bands, which occurs after 12 minutes and continues until equilibrium is attained approximately 30 minutes after initial mixing of the solutions (Figure 3b). These results are consistent with circular dichroism (CD) spectroscopy data that show a strongly split Cotton effect with positive and negative signals at 486 and 493 nm, respectively (Figures S7 and S8).[12]

Based on these observations, we propose the following mechanism for formation of the porous multi-chambered peptide-porphyrin microspheres (Figure 3c). Initially, dipeptide-mediated charge screening of the nucleated J-aggregates in combination with stoichiometric packing of $[FF]^+$ cations specifically around the supramolecular porphyrin architecture promotes the formation of peptide–porphyrin ionic complexes that self-assemble into nanorods with characteristic chiral amplification (Figure S9a,b). The nanorods then undergo higher-order aggregation into the porous microspheres (Figure S9c,d in the Supporting Information), possibly through a combination of electrostatic and π–π stacking interactions involving the phenylalanine side chains of the dipeptide. The primary involvement of electrostatically mediated co-assembly is confirmed by facile disassembly of the microspheres under conditions of increased ionic strength (Figure S10). Moreover, replacing $[H_4TPPS]^{2-}$ with FeTPPS (Figure S1 in the Supporting Information), which does not undergo supramolecular stacking, produced no microspheres when solutions were acidified in the presence of cationic dipeptide.

Given the plausible pre-biotic relevance of small peptides and water-soluble porphyrins, the ability of such molecules to undergo spontaneous co-assembly into highly hydrated multi-chambered microspheres inspire us to investigate these porous materials as a new type of photoactive protocell model based on membrane-free compartmentalization. As a first step, we investigate the sequestration properties and photocatalytic activity of the peptide–porphyrin microspheres. Organic molecules are sequestered or excluded from the microspheres depending on their charge. For example, uptake of positively charged rhodamine dyes is rapid and extensive (ca. 70 wt% in the case of rhodamine 6G) (Figure S11a,b). Also, amino acids such as tryptophan and Fmoc-lysine bearing positive charge under acidic conditions are sequestered into the microspheres. In contrast, negatively charged small organic molecules such as 2,6-naphthalenedisulfonate or flavin adenine dinucleotide are essentially excluded from the interior of the peptide–porphyrin microspheres. We attribute the differences in uptake to the high negative surface potential of the microspheres (zeta potential, −28.6 mV), which specifically inhibited the sequestration of negatively charged solutes because of electrostatic repulsion at the water–particle interface. A similar charge-mediated selectivity is observed for the uptake of polyelectrolytes; for example, positively charged polylysine ($M_w = 15$–30 kDa) is readily sequestered into

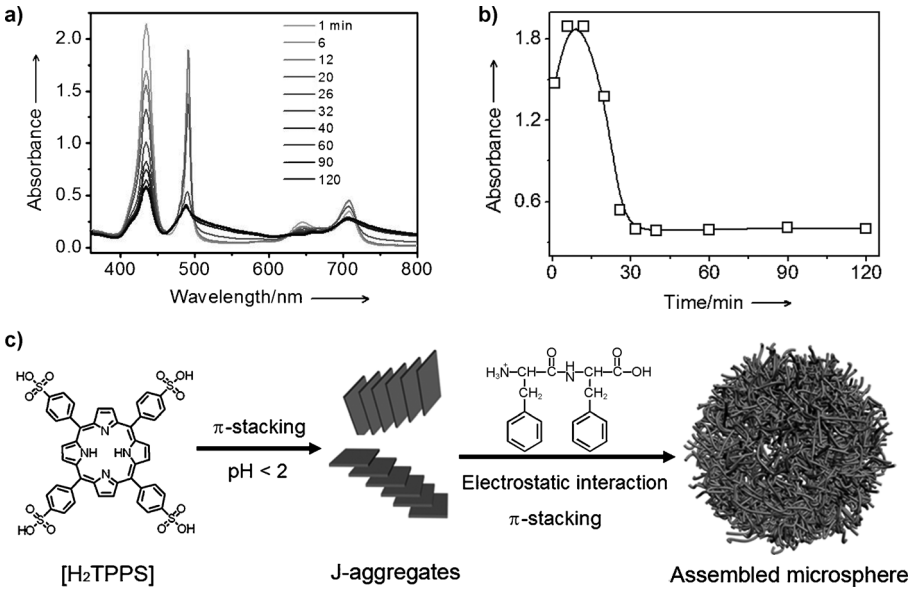

Figure 3. Mechanism of peptide–porphyrin microsphere self-assembly. a) Time-dependent UV/Vis spectra showing formation of peptide–porphyrin microspheres as evidenced by changes in the intensities of peaks at 434 and 490 nm. b) Plot of absorbance intensity at 490 nm versus time showing initial formation of J-aggregate superstructures followed by broadening and decreasing the intensity of the spectral peak because of interactions between $[FF]^+$ and the J-aggregate nanorods. c) Possible mechanism for the self-assembly of peptide–porphyrin microspheres, involving dipeptide-mediated charge screening of the porphyrin J-aggregates in combination with local stacking of dipeptide cations specifically around the J-aggregates.

the peptide–porphyrin microspheres (Figure S11c), whilst negatively charged single-stranded DNA ($M_w = 9200$) is excluded from the interior of the colloid.

To test whether photocatalytic transformations could be supported in the presence of the porous multi-chambered microspheres, we investigated the light-induced oxidation of iodide to tri-iodide in acidic aqueous solution (Scheme S1).[16] Increases in peak intensity at $\lambda = 353$ and 287 nm in the time-dependent UV/Vis absorption spectra are associated with I_3^- production and used to monitor the reaction rate (Figure 4a). Photocatalytic oxidation is maintained in the presence of the microspheres although the reaction rate is slightly reduced compared with a dispersion of pure J-aggregates (Figure 4b). Interestingly, the microspheres possess considerable stability against photodegradation compared to the native J-aggregates when irradiated for extended periods of time, as evidenced by minimal changes in the Soret and Q band intensities (Figure 4a,b). In contrast, under the same conditions the native J-aggregates show decreases of ca. 36% and 27% in the Soret and Q band intensities, respectively (Figure S12). Thus, the yield of iodide is maintained over longer periods of time (> 5 h) in the presence of the microspheres, suggesting that binding of $[FF]^+$ to the stacked $[H_4TPPS]^{2-}$ dianions, or the structural stability of the microstructured matrix, or both, are possible factors responsible for the sustained catalytic performance.

We also investigated the potential of the porous multi-chambered microspheres as photosynthetic prototypes for the catalytic reduction of metal salts in aqueous media. For this, we exploited the potential of porphyrins to capture light to produce photoexcited states that are rapidly reduced by an electron donor such as ascorbic acid. The resulting porphyrin radical anion can then be used catalytically to reduce various metal salts to the metallic state through a succession of light harvesting and photochemical cycles (Scheme S2). We tested whether such reactions would remain active in the presence of the peptide-porphyrin complex of the porous microspheres by addition of aqueous K_2PtCl_4 (final concentration, 1 mM) and ascorbic acid to a dispersion of the peptide–porphyrin microspheres. TEM investigations indicate that photoreduction of the Pt^{II} salt occurs within 5 min of irradiation (as evidenced visibly by color change from green to dark green) to produce microspheres surface-decorated with discrete Pt nanoparticles approximately 2 nm in size (Figure 4c). Control experiments without light irradiation or in the absence of the microspheres show no nanoparticle formation, indicating that the reaction proceeded photocatalytically in the presence of the peptide–porphyrin microstructure. It is also possible to prepare microspheres encased in high concentrations of Pt nanoparticles by increasing the K_2PtCl_4 concentration above a value of 3 mM (Figure S13). Under these conditions, microsphere-mediated photocatalytic reduction and nucleation of the Pt clusters appear to be augmented by autocatalytic reduction on the surface of the preformed Pt nanoparticles as they attain a critical size.[17]

The versatility of the porous peptide–porphyrin microspheres for photocatalytic reduction is demonstrated by applying the above methodology in the presence of small organic molecules. As proof-of-principle, we irradiated the microspheres in a solution containing 4-nitrophenol (4-NP) for periods of up to 150 min, and detected spectroscopically the time-dependent changes in the concentration of 4-NP and the photoreduced product, 4-aminophenol (4-AP; Figure 4d and Figure S14a). The time-dependant spectra reveal a reaction rate of 5.5×10^{-5} mM min^{-1} (Fig-

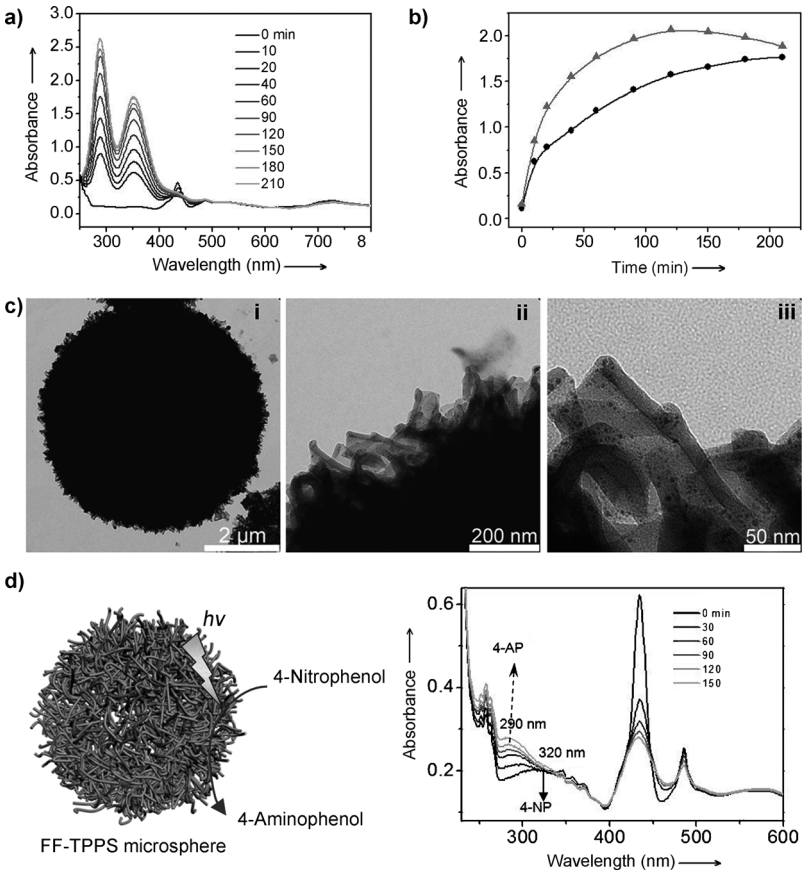

Figure 4. Use of porous multi-chambered peptide–porphyrin microspheres in photocatalysis. a) UV/Vis adsorption spectra showing time-dependent changes in peak intensities at $\lambda = 353$ and 287 nm corresponding to product formation under constant irradiation of sodium iodide (initial $[I^-] = 5$ mM). b) Plots of absorption intensity at A_{353} versus irradiation time for tri-iodide formation in the presence of a dispersion of the microspheres (black) or $[H_4TPPS]^{2-}$ J-aggregates (gray). c) Photocatalytic reduction of Pt^{II} and nucleation of Pt nanoparticles on the surface of peptide–porphyrin microspheres; TEM images of a single microsphere (i), and at higher magnification (ii,iii) showing discrete, electron dense Pt nanoparticles associated with the peptide–porphyrin nanorod substructure. d) Photocatalytic reduction of 4-nitrophenol (4-NP) into 4-aminophenol (4-AP) in the presence of a dispersion of the microspheres; the UV/Vis spectra (right) show a time-dependent increase in peak intensity at 290 nm, corresponding to the production of 4-AP.

ure S14b). A control experiment without addition of the microspheres shows no changes in the absorption peaks before and after exposure to light (Figure S14c), confirming that the microspheres act as a photosynthetic system for the photocatalytic reduction of 4-NP into 4-AP.

In conclusion, photocatalytically active microspheres with highly hydrated, accessible multi-chambered interiors have been prepared by cooperative self-assembly of simple dipeptides and porphyrins. The colloidal microspheres comprise a network of J-aggregate nanoscale substructures that serve as light-harvesting antennae with a relatively broad spectral cross-section and considerable photostability. These optical properties can be exploited in photocatalytic reactions involving inorganic or organic species. Taken together, these structural and functional features suggest that soft porous biomolecule-based colloids are a plausible photosynthetic model that could be developed towards demonstrating aspects of primitive abiotic cellularity. Whilst we do not consider the dipeptide and porphyrin system to be highly plausible candidates per se for the origin of photosynthetic aggregates on the early Earth, the underlying structural and functional features of the synthetic peptide–porphyrin microspheres could have general mechanistic relevance for the study of energy capture and conversion in prebiotic chemistry.

Received: October 9, 2013
Revised: November 29, 2013
Published online: January 31, 2014

Keywords: peptides · porous colloids · porphyrins · primitive photosynthetic model · self-assembly

[1] a) J. B. Li, Q. He, X. H. Yan, *Molecular Assembly of Biomimetic Systems*, Wiley, Hoboken, **2011**; b) R. V. Ulijn, D. N. Woolfson, *Chem. Soc. Rev.* **2010**, *39*, 3349 – 3350; c) S. Mann, *Acc. Chem. Res.* **2012**, *45*, 2131 – 2141; d) K. Ariga, J. P. Hill, M. V. Lee, A. Vinu, R. Charvet, S. Acharya, *Sci. Technol. Adv. Mater.* **2008**, *9*, 014109; e) H. G. Cui, E. T. Pashuck, Y. S. Velichko, S. J. Weigand, A. G. Cheetham, C. J. Newcomb, S. I. Stupp, *Science* **2010**, *327*, 555 – 559; f) Z. Z. Lin, X. C. Wang, *Angew. Chem.* **2013**, *125*, 1779 – 1782; *Angew. Chem. Int. Ed.* **2013**, *52*, 1735 – 1738.

[2] a) J. W. Szostak, D. P. Bartel, P. L. Luisi, *Nature* **2001**, *409*, 387 – 390; b) S. Zhang, *Acc. Chem. Res.* **2012**, *45*, 2142 – 2150; c) J. W. Szostak, *Nature* **2009**, *459*, 171 – 172.

[3] a) B. Städler, A. D. Price, R. Chandrawati, L. Hosta-Rigau, A. N. Zelikin, F. Caruso, *Nanoscale* **2009**, *1*, 68 – 73; b) P. Stano, P. Carrara, Y. Kuruma, T. P. de Souza, P. L. Luisi, *J. Mater. Chem.* **2011**, *21*, 18887 – 18902; c) S. Mann, *Angew. Chem.* **2013**, *125*, 166 – 173; *Angew. Chem. Int. Ed.* **2013**, *52*, 155 – 162.

[4] M. M. Hanczyc, S. M. Fujikawa, J. W. Szostak, *Science* **2003**, *302*, 618 – 622.

[5] S. S. Mansy, J. P. Schrum, M. Krishnamurthy, S. Tobé, D. A. Treco, J. W. Szostak, *Nature* **2008**, *454*, 122 – 125.

[6] a) P. M. Gardner, K. Winzer, B. G. Davis, *Nat. Chem.* **2009**, *1*, 377 – 383; b) R. Krishna Kumar, X. Yu, A. J. Patil, M. Li, S. Mann, *Angew. Chem.* **2011**, *123*, 9515 – 9519; *Angew. Chem. Int. Ed.* **2011**, *50*, 9343 – 9347; c) K. Kurihara, M. Tamura, K.-i. Shohda, T. Toyota, K. Suzuki, T. Sugawara, *Nat. Chem.* **2011**, *3*, 775 – 781; d) V. Noireaux, A. Libchaber, *Proc. Natl. Acad. Sci. USA* **2004**, *101*, 17669 – 17674.

[7] a) X. Huang, M. Li, D. C. Green, D. S. Williams, A. J. Patil, S. Mann, *Nat. Commun.* **2013**, *4*, 2239; b) W. Tong, C. Gao, H. Möhwald, *Colloid Polym. Sci.* **2008**, *286*, 1103 – 1109; c) D. Mertz, J. Cui, Y. Yan, G. Devlin, C. Chaubaroux, A. Dochter, R. Alles, P. Lavalle, J. C. Voegel, A. Blencowe, *ACS nano* **2012**, *6*, 7584 – 7594.

[8] a) M. Li, D. C. Green, J. R. Anderson, B. P. Binks, S. Mann, *Chem. Sci.* **2011**, *2*, 1739 – 1745; b) R. K. Kumar, M. Li, S. N. Olof, A. J. Patil, S. Mann, *Small* **2013**, *9*, 357 – 362.

[9] P. Walde, S. Ichikawa, *Biomol. Eng.* **2001**, *18*, 143—177.

[10] a) S. Koga, D. S. Williams, A. W. Perriman, S. Mann, *Nat. Chem.* **2011**, *3*, 720 – 724; b) D. S. Williams, S. Koga, C. R. C. Hak, A. Majrekar, A. J. Patil, A. W. Perriman, S. Mann, *Soft Matter* **2012**, *8*, 6004 – 6014.

[11] X. H. Yan, P. L. Zhu, J. B. Li, *Chem. Soc. Rev.* **2010**, *39*, 1877 – 1890.

[12] J. M. Ribó, J. Crusats, F. Sagués, J. Claret, R. Rubires, *Science* **2001**, *292*, 2063 – 2066.

[13] a) M. Fishkis, *Origins Life Evol. Biospheres* **2007**, *37*, 537 – 553; b) M. Kolesnikov, I. Egorov, *Origins Life* **1977**, *8*, 383 – 390.

[14] a) Y. Matsuzawa, K. Ueki, M. Yoshida, N. Tamaoki, T. Nakamura, H. Sakai, M. Abe, *Adv. Funct. Mater.* **2007**, *17*, 1507 – 1514; b) A. Barth, C. Zscherp, *Q. Rev. Biophys.* **2002**, *35*, 369 – 430.

[15] a) E. B. Fleischer, J. M. Palmer, T. Srivastava, A. Chatterjee, *J. Am. Chem. Soc.* **1971**, *93*, 3162 – 3167; b) R. F. Pasternack, P. R. Huber, P. Boyd, G. Engasser, L. Francesconi, E. Gibbs, P. Fasella, G. Cerio Venturo, L. d. Hinds, *J. Am. Chem. Soc.* **1972**, *94*, 4511 – 4517; c) B. J. Pepe-Mooney, B. Kokona, R. Fairman, *Biomacromolecules* **2011**, *12*, 4196 – 4203; d) O. Ohno, Y. Kaizu, H. Kobayashi, *J. Chem. Phys.* **1993**, *99*, 4128 – 4139; e) A. D. Schwab, D. E. Smith, C. S. Rich, E. R. Young, W. F. Smith, J. C. de Paula, *J. Phys. Chem. B* **2003**, *107*, 11339 – 11345.

[16] L. Slavětínská, J. Mosinger, P. Kubát, *J. Photochem. Photobiol. A* **2008**, *195*, 1 – 9.

[17] Z. C. Wang, C. J. Medforth, J. A. Shelnutt, *J. Am. Chem. Soc.* **2004**, *126*, 16720 – 16721.

